

## The effect of solar spectral irradiance and temperature on the electrical characteristics of a ZnO-SiO<sub>2</sub>-Si (N) photovoltaic structure

Fayçal Bouzid\* et Samira Ben Machich

Faculty of Sciences, El Hadj Lakhdar University, Batna, Algeria

(reçu le 06 Septembre 2009 – accepté le 25 Juin 2010)

**Abstract** - The aim of this article is to present an analytic study of the impact of changing solar spectrum and temperature on the performance and electrical characteristics of a MIS solar cell. With this intention, one simulation of the spectral response and the current-voltage characteristic was carried out using a simulation program designed under 'Visual Basic 5' language for this reason. Our study is made on a ZnO-SiO<sub>2</sub>-Si (N) solar cell; it proves that the spectral response has higher collection efficiency for carriers generated by ultraviolet light and a conversion efficiency of about 18 % can be obtained under AM1 solar spectrum and at ambient temperature. The results presented indicate also that the increase in solar cell's temperature results a degradation of their performances.

**Résumé** - Le but de cet article est de présenter une étude analytique de l'impact du changement du spectre solaire et de la température sur les performances et les caractéristiques électriques d'une cellule solaire de type MIS. Pour ce faire, une simulation de la réponse spectrale et de la caractéristique courant-tension a été effectuée en utilisant un programme de simulation développé sous langage 'Visual Basic 5' pour cette raison. Notre étude est faite sur une cellule solaire de type ZnO-SiO<sub>2</sub>-Si (N); cette étude prouve que la réponse spectrale a une efficacité de collection plus élevée pour les porteurs produits par la lumière ultraviolette ainsi qu'une efficacité de conversion environ de 18 % peut être obtenue sous le spectre solaire AM1 pour la température ambiante. Les résultats présentés indiquent également que l'augmentation de la température de la cellule provoque une dégradation de ses performances.

**Keywords:** MIS solar cell - Solar spectrum - Spectral response – I (V) characteristics - Temperature.

### 1. INTRODUCTION

One possibility of making solar cell arrays cheaply lies in the fabrication techniques and design. One of these techniques is the application of an ultra-thin metal or a relatively thick transparent conducting metal on the surface of the semiconductor.

However, it was shown by a number of experimental investigations that a thin insulator layer between the metal and the semiconductor (N or P type) has an especially strong influence on the electrical characteristics. Several experimental and theoretical results have already indicated the possibility of fabricating MIS solar cells with efficiencies up to 18 % at AM1 irradiance [1].

For the application of this kind of photovoltaic structure, i.e. the planning of photovoltaic systems, the knowledge of the conversion efficiency under varying operating conditions (Temperature, Illumination) is of crucial importance. To optimize

---

\* seifay@yahoo.com

solar cells at realistic operating conditions and to analyze system performance, the variation of physical parameters of silicon (Si) with temperature is needed.

Even at a given level of irradiance, the temperature of individual cells can range from -15 to 80 °C during the course of a year, leading to significant variations in the cell output. The purpose of this paper is to analyze the effect of varying operating conditions on a ZnO-SiO<sub>2</sub>-Si (N) solar cell, using a simulation program designed to simulate the effect of changing the physical and geometrical parameters, temperature and irradiance on MIS solar cells.

## 2. THEORETICAL BACKGROUND

In this work, the metal chosen for our structure subject is the Zinc oxide (ZnO). It is a material that belongs to the family of transparent conductive oxides (TCO). Its non-toxicity and the abundant availability in the Earth's crust of its components make it an ideal candidate as electrical transparent contact for thin-film amorphous and/or microcrystalline Silicon solar cells [2].

The Low-Pressure Chemical Vapour Deposition (LP-CVD) method allows one to obtain rough (ZnO) layers, which can effectively scatter the light that passes through them. This high scattering capacity increases the path of the light within the solar cell and therefore enhances its probability to be absorbed by the solar cell, and consequently the photo-generated current.

Zinc oxide (ZnO) has a work function of 4.95 [eV] for the oxygen terminated (ZnO) (000 $\bar{1}$ ) surface, which is in good agreement with the values obtained for films deposited with  $\geq 5\%$  oxygen in the sputter gas [3]. Further, its refractive index is about 2.2 [4], so it can be used as an anti reflection coating.

The energy band diagram of our structure subject under forward bias condition is shown in (Fig. 1.). The difference between the metal and the semiconductor work functions generate an electric field which is responsible of the hole-electron separation.

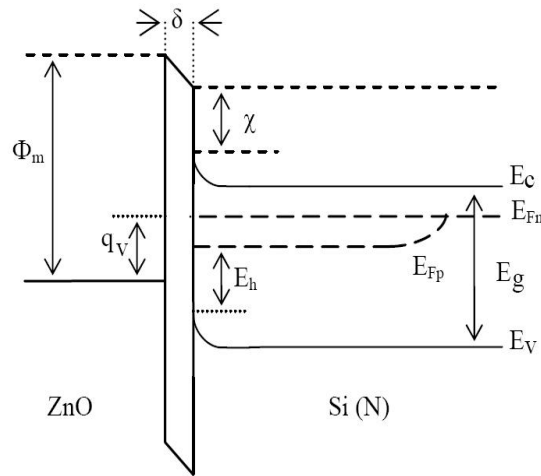


Fig. 1: Energy band diagram of a ZnO-SiO<sub>2</sub>-Si (N) solar cell under illumination

The photovoltaic literature has contained papers describing several models used to investigate the solar cells performance. In our program, a complete set of equations is used which include the important carrier transport mechanisms.

For N-type crystalline Silicon cells, the total output current drawn under illumination is given by [5] as:

$$I_{\text{Total}} = I_{\text{Light}} - I_{\text{Dark}} \quad (1)$$

## 2.1 Dark current

For thin film MIS solar cells, the most probable current transport mechanisms in dark are field emission (tunneling), minority carrier diffusion and carrier recombination. The dark current can be expressed as [6, 7]:

$$I_{\text{Dark}} = I_{\text{eto}} \left[ \exp \frac{q v_s}{n k T} - 1 \right] + I_{\text{do}} \left[ \exp \frac{q (v_s + \Delta)}{k T} - 1 \right] + I_{\text{ro}} \left[ \exp \frac{(E_{\text{Fn}} - E_{\text{Fp}})}{2 k T} - 1 \right] \quad (2)$$

where  $I_{\text{eto}}$ ,  $I_{\text{do}}$  and  $I_{\text{ro}}$  are the reverse saturation currents associated with electron tunneling, hole diffusion, and recombination mechanisms respectively,  $E_{\text{Fn}}$  and  $E_{\text{Fp}}$  are the electron and hole quasi-Fermi levels,  $k$  is the Boltzmann constant,  $T$  is the temperature and  $v_s$  is the voltage across the depletion region width of the semiconductor.

$$\Delta = E_g - \phi_{\text{bn}} - E_h \quad (3)$$

where  $E_g$  is the band gap energy,  $E_h$  is the minority carrier quasi-Fermi level, and  $\phi_{\text{bn}}$  is the Schottky barrier height for N-type (Si). It is expressed as [7]:

$$\phi_{\text{bn}} = \gamma \phi_{\text{bo}} + (1 - \gamma)(E_g - \phi_0) \quad (4)$$

where:

$$\phi_{\text{bo}} = \phi_m - \chi \quad (5)$$

$$\gamma = 1 / (1 + \alpha) \quad (6)$$

$$\alpha = (q D_{\text{ss}} \delta) / (\xi_i) \quad (7)$$

$\phi_m$  is the work function of the metal,  $\phi_0$  is the level above the valence band to which surface states are filled in isolated semiconductor,  $\chi$  is the electronic affinity of Silicon,  $D_{\text{ss}}$  is the interface state density,  $\xi_i$  is the permittivity of the interfacial oxide layer ( $\text{SiO}_2$ ),  $\delta$  is the thickness of the oxide layer.

The ideality factor  $n$  is related to the oxide thickness and interface states density by the relation proposed by Card et al. [8] as:

$$n = 1 + \left[ \frac{\xi_s}{w} + q \cdot D_{\text{ss}} \right] \cdot \frac{\delta}{\xi_i} \quad (8)$$

$\xi_s$  is the permittivity of Silicon.

The reverse saturation currents are given by [6, 7] as:

$$I_{eto} = A * S T^2 \exp(-\sqrt{\chi} \cdot \delta) \exp(-q \phi_{bn} / k \cdot T) \quad (9)$$

Where  $A^*$  is the effective Richardson's constant and  $S$  is the surface of the cell.

$$I_{do} = \frac{q n_i^2 S}{N_d} \cdot \left\{ \left[ S_p \coth\left(\frac{d-w}{L_p}\right) + \frac{D_p}{L_p} \right] / \left[ \left(\frac{d-w}{L_p}\right) + \frac{S_p L_p}{D_p} \right] \right\} \quad (10)$$

$$I_{ro} = \frac{q n_i^2 S w}{2 \tau_p} \quad (11)$$

where  $n_i$  is the intrinsic carrier concentration,  $N_d$  is the doping concentration,  $S_p$  is the surface recombination velocity of holes at the back surface,  $D_p$ ,  $L_p$  and  $\tau_p$  are the minority carrier diffusion constant, length constant and life time respectively,  $d$  is the cell thickness and  $w$  is the depletion layer width, it is given by [1, 6] as:

$$w = \left[ \frac{2 \xi_s}{q N_d} \left( v_{bi} - v_s - \frac{k T}{q} \right) \right]^{1/2} \quad (12)$$

where  $v_{bi}$  is the built in voltage.

## 2.2 Photocurrent

The photocurrent generated in the bulk and in the transition region is given by:

$$I_{Light} = \int_{\lambda_{min}}^{\lambda_g} [I_{dl}(\lambda) + I_{pw}(\lambda)] \cdot d\lambda \quad (13)$$

where  $I_{dl}(\lambda)$  is the contribution of carriers generated in the depletion layer,  $I_{pw}(\lambda)$  is the contribution of the diffusion of holes at the depletion layer boundary,  $\lambda_{min}$  is the minimum wavelength of the solar spectrum and  $\lambda_g$  is the wavelength corresponding to the Silicon energy gap.

For monochromatic illumination  $I_{dl}$  can be written as:

$$I_{dl}(\lambda) = \int_0^w G(x, \lambda) dx \quad (14)$$

where,  $G(x, \lambda)$  is the optical electron – hole pair generation rate, it is expressed as [5]:

$$G(x, \lambda) = \left[ \frac{S \alpha(\lambda) N(\lambda)}{1 - r_f \cdot r_b \exp(-2 \alpha d)} \right] \times (\exp(-\alpha x) + r_b \exp(-\alpha(2d - x))) \quad (15)$$

where,  $\alpha(\lambda)$  is the semi-conducteur absorption,  $N(\lambda)$  is the photon flux density of the solar spectrum,  $r_f$  and  $r_b$  are the reflection coefficient at the front and back surfaces respectively.

$$I_{dl}(\lambda) = \left[ \frac{SqN(\lambda)}{1 - r_f \cdot r_b \exp(-2\alpha d)} \right] \cdot \{1 - \exp(-\alpha w) + r_b \exp(-\alpha(2d-w)) - r_b \exp(-2\alpha d)\} \quad (16)$$

By solving the hole continuity equation we obtain the expression of  $I_{pw}(\lambda)$ :

$$I_{pw}(\lambda) = \frac{qL_p S}{\alpha^2 L_p^2 - 1} \left\{ -L_p G'(w, \lambda) + \frac{\left[ S'_p G(d, \lambda) + L_p G'(d, \lambda) \right] - \left[ G(w, \lambda) (S'_p \cosh v_p + \sinh v_p) \right]}{S'_p \sinh v_p + \cosh v_p} \right\} \quad (17)$$

where

$$G'(x, \lambda) = \frac{\partial G(x, \lambda)}{\partial x} \quad (18)$$

$$S'_p = \frac{S_p L_p}{D_p} \quad (19)$$

$$v_p = \frac{d - w}{L_p} \quad (20)$$

For indirect transitions, light absorption is assisted by the absorption or emission of phonons. Theory predicts the absorption coefficient of crystalline Silicon to be [9]:

$$\alpha(T) = \sum_{i,j=1,2} A_j C_i \times \left\{ \frac{(\hbar\nu - E_{g,j} + E_{ph,i})^2}{\exp\left(\frac{E_{ph,i}}{kT}\right) - 1} + \frac{(\hbar\nu - E_{g,j} + E_{ph,i})^2}{1 - \exp\left(\frac{E_{ph,i}}{kT}\right)} \right\} + A_d \cdot \frac{(\hbar\nu - E_{gd})^{3/2}}{\hbar\nu} \quad (21)$$

Where,  $i$  and  $j$  are the photons 1, 2 and bands gaps 1, 2 respectively.  $E_{g,1} = 1.1$  (eV) and  $E_{g,2} = 2.25$  (eV) are the indirect band gaps 1 and 2, and  $E_{g,d} = 3.2$  (eV) is the direct band gap 3 with all values for  $T$  (K) being.  $E_{ph,1} = 212 \times k$  and  $E_{ph,2} = 670 \times k$  are the phonons with  $C_1 = 5.5$ ,  $C_2 = 4$  and  $A_1 = 253$ ,  $A_2 = 3312$  and  $A_d = 2.3 \times 10^7$  in  $(\text{cm}^{-1} \text{eV}^{-2})$ .

The first term describes the absorption of phonons while the second describes the emission of phonons during absorption of light. The third term gives the absorption for a direct transition.

### 2.3 Spectral response

The term spectral response is related to the light generated current and the wavelength of the incident monochromatic light. It is simply the output current under short circuit conditions at each wavelength divided by the light power incident on the cell. It can be written as [1]:

$$SR(\lambda) = j_{sc} / P_{inc}$$

where,  $j_{sc}$  is the short circuit density and  $p_{inc}$  is the total incident solar power.

## 2.4 Photovoltaic parameters

The open circuit voltage is given by [1] as:

$$V_{oc} = n \left[ \phi_{bn} + \frac{kT}{q} \sqrt{\chi} \delta + \frac{kT}{q} \ln \left( \frac{I_{sc}}{SA^* T^2} \right) \right] \quad (23)$$

Where  $I_{sc}$  is the short circuit current.

The cell output power, assuming negligible series resistance, is given as:

$$p = I_{Total} \times v \quad (24)$$

Where  $v$  is the applied voltage and the cell conversion efficiency is usually taken to be:

$$\eta = \frac{I_m \times v_m}{P_{inc}} \quad (25)$$

Where  $I_m$  and  $v$  are coordinates of the maximum power point. The fill factor is defined by:

$$FF = \frac{I_m \times v_m}{I_{sc} \times v_{oc}} \quad (26)$$

## 3. RESULTS AND DISCUSSION

The reflection coefficient of  $\text{SiO}_2$  coated Silicon is 0.15, and for uncoated Silicon it is 0.3 [10]. In our model, the reflection coefficients at the front and back surfaces are assumed to be 0.2 and 0.5 respectively. The values assigned for the cell parameters are presented in **Table 1**.

**Table 1:** Parameters of the cell

Parameters	Nd	d	S	$\delta$	$\phi_m$	$\phi_m$	$\phi_0$	S <sub>p</sub>	$\tau_p$
Values	3 e18	0.0025	1.5	5 e-8	1 e12	4.95	0.35	1 e2	7 e-6

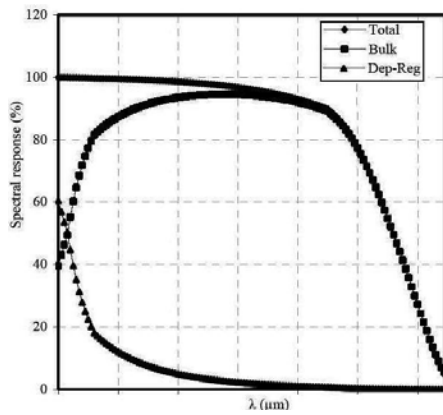


Fig. 2.a: The total spectral response and its components under AM0 at 27 °C

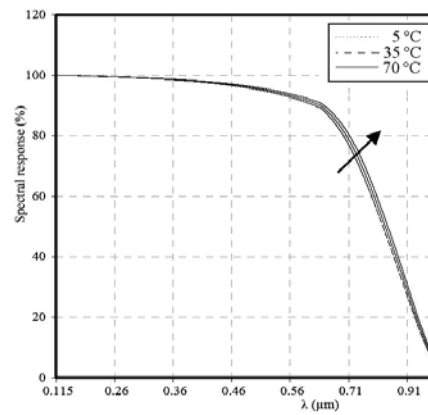


Fig. 2.b: The effect of the temperature on the total spectral response under AM0

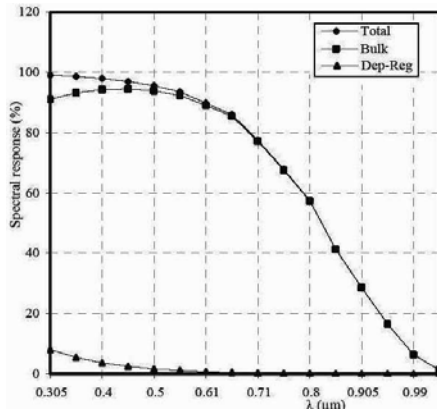


Fig. 3.a: The total spectral response and its components under AM1 at 27 °C

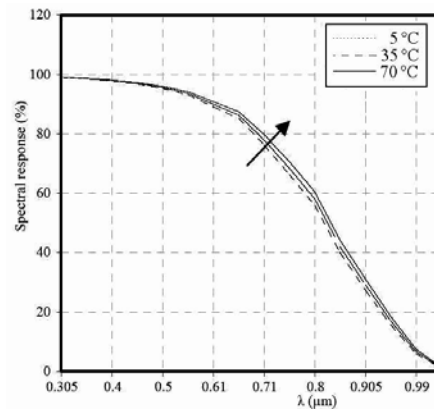


Fig. 3.b: The effect of the temperature on the total spectral response under AM1

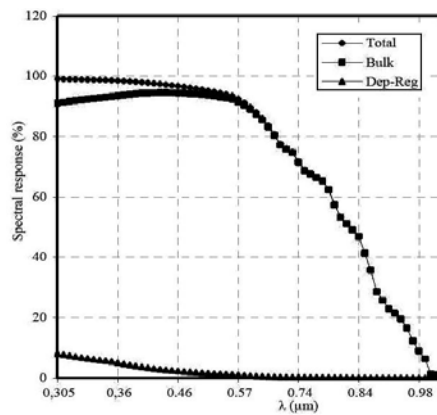


Fig. 4.a: The total spectral response and its components under AM2 at 27 °C

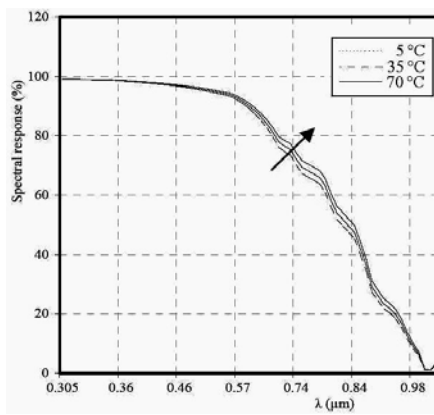


Fig. 4.b: The effect of the temperature on the total spectral response under AM2

### 3.1 Effect of different solar spectrum on the spectral response

The spectral response of the solar cell has been simulated for different solar spectrum. Figures (2.a, 3.a and 4.a) show the detailed spectral responses of the solar cell with the total response under illuminations AM0, AM1 and AM2 respectively.

The results presented in these figures indicate that the distributions of the two components (depletion region and bulk) are complementary; the cell has higher collection efficiency for carriers generated by ultraviolet light and it has a poor red response (longer wavelengths).

The relative importance of the two components depends mainly on the diffusion length, the rear surface recombination velocity, and the absorption coefficient  $\alpha(\lambda)$  [11].

The diffusion length severely affects the cells' response, since the free carriers generated deeper in the bulk have to travel longer before being collected. This results a higher recombination loss. The diffusion length is determined by the quality of the Silicon. It depends on the technology and in particular on the methods employed for doping.

The absorption coefficient  $\alpha(\lambda)$  decreases with the increasing of the photons wavelengths, so the loss in absorption causes the spectral response to decrease quickly.

It may be seen, as comparison between the three responses, that the reduction in illumination intensity causes a reduction in the short circuit current for longer wavelengths, which explains the reduction that undergoes the spectral response.

### 3.2 Effect of temperature on the spectral response

**Tableau 2:** Effect of temperature on some physical parameters

Temperature	Lp (cm)	Dp (cm <sup>2</sup> /s)	$\tau_p$ (s)	$\mu_p$ (cm <sup>2</sup> /v.s)	n
5 °C	0.0097	12.92	0.0000073	539.05	1.106
35 °C	0.0089	11.61	0.0000069	437.29	1.106
70 °C	0.0082	10.42	0.0000065	352.21	1.107

The figures (2.b, 3.b and 4.b) above represent the variation of the spectral response of our solar cell with temperature, which varies in the interval 5 °C – 70 °C for AM0, AM1 and AM2 solar spectrum.

As a consequence of the increase in temperature, there is a shift in the spectral response curves. According to the results represented in **Table 2** and the preceding curves, we note that when the temperature of the cell increases, the thermal agitation of the crystal lattice becomes intense, which causes a reduction in the mobility and the minority carriers lifetime and, consequently, a reduction in the diffusion lengths, as well as the mechanism of recombination of the carriers becomes stronger.

In addition, the increase in the temperature causes a reduction in the band gap width; therefore the mechanism of production of carriers becomes increasingly significant.

For relatively low or middling temperatures (the case of our study), there is an equilibrium between these two mechanisms (generation and recombination). But when one takes into account the behaviour of the absorption coefficient of Silicon according to the temperature, one manages to explain the shift observed on the three curves.

Owing to the fact that absorption in silicon, for long wavelengths, is more significant in the bulk, and that it improves as the temperature increases because of the phonons multiplication phenomenon [12], the minority carriers production mechanism will dominate the mechanism of recombination in this range of long wavelengths, that wants to say that the photocurrent increases and, consequently, the spectral response.

In addition, the shift observed towards the long wavelengths is because of the shift of the threshold of absorption of Silicon towards low energies with the increase in temperature [13].

### 3.3 Effect of different solar spectrum on the I - V characteristics

The figure above show the I - V characteristics and the powers delivered by the ZnO-SiO<sub>2</sub>-Si(N) solar cell illuminated by AM0, AM1 and AM2 solar spectrum



respectively. This figure as well as the table above allows the comparison of the characteristics calculated in three cases of illumination.

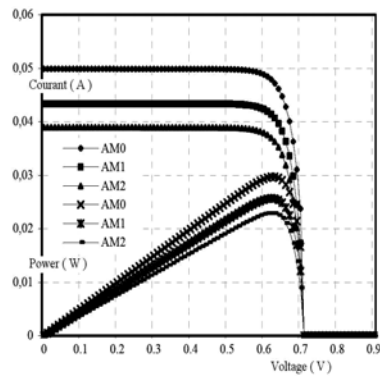


Fig. 5: I-V characteristics and powers delivered under different solar spectrum

**Table 3:** Photovoltaic parameters under different solar spectrum at 27 °C

AM	$P_{inc}$	$V_{oc}$	$I_{sc}$	FF	$\eta$	$P_{max}$
0	0.1358	0.72	0.05	82.83	14.5	0.0297
1	0.0971	0.715	0.043	83.74	17.6	0.0256
2	0.0768	0.712	0.039	82.65	19.9	0.0229

It is thus observed that the reduction in the intensity of irradiation involves a reduction in the photocurrent because, as we saw in equations (16, 17), the photocurrent is practically proportional to luminous flow and owing to the fact that the open circuit voltage is also related to the short circuit current, it will undergo a small reduction as it is indicated in (Table 3) above.

The conversion efficiency is always better in AM2 than in AM0, but the provided maximum power is lower.

### 3.4 Effect of temperature on the I - V characteristics

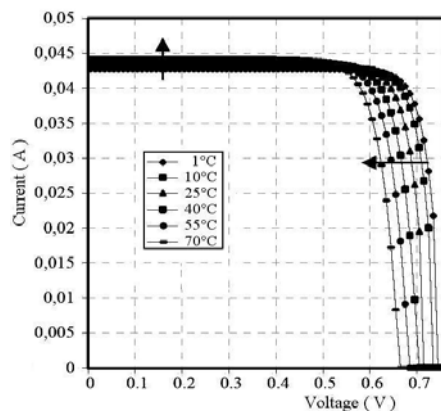


Fig. 6: I - V characteristics for different temperatures under solar spectrum AM1

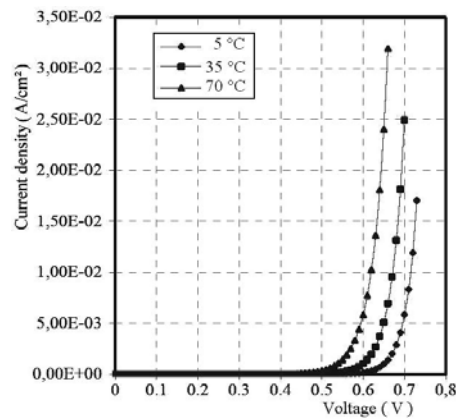
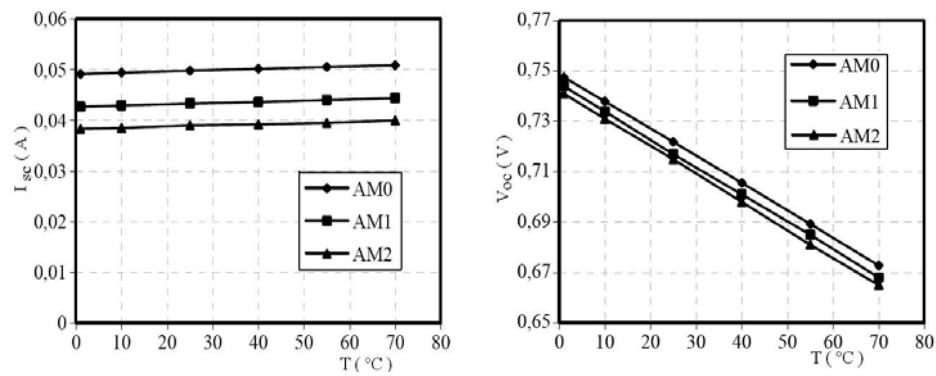
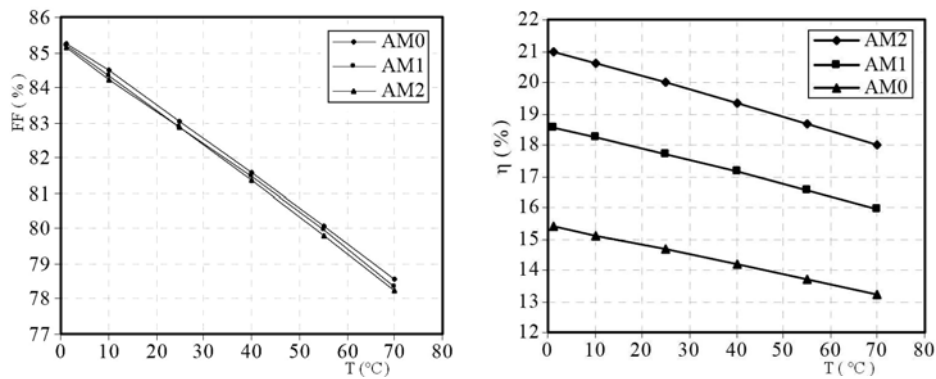


Fig. 7: I - V characteristics for different temperatures in dark

**Table 4:** Variation of the photovoltaic parameters of the ZnO-SiO<sub>2</sub>- Si (N) Solar Cell with the Solar Spectrum and Temperature

T AM	1°C			10°C			25°C		
	0	1	2	0	1	2	0	1	2
I <sub>sc</sub>	0.0491	0.0427	0.0383	0.0494	0.0429	0.0385	0.0498	0.0433	0.039
V <sub>oc</sub>	0.747	0.744	0.741	0.738	0.734	0.731	0.722	0.717	0.715
I <sub>FF</sub>	85.24	85.19	85.12	84.46	84.35	84.24	83.06	82.88	82.85
η	15.37	18.57	20.98	15.11	18.24	20.60	14.65	17.69	19.98
T AM	40°C			55°C			70°C		
	0	1	2	0	1	2	0	1	2
I <sub>sc</sub>	0.050	0.0436	0.0392	0.0505	0.044	0.0395	0.051	0.0444	0.04
V <sub>oc</sub>	0.705	0.701	0.698	0.689	0.685	0.681	0.672	0.668	0.655
I <sub>FF</sub>	81.58	81.46	81.37	80.06	79.95	79.81	78.54	78.37	78.22
η	14.18	17.13	19.33	13.69	16.54	18.66	13.20	15.94	17.97

**Fig. 8:** Variations of the short circuit current and the open circuit voltage with the solar spectrum and temperature**Fig. 9:** Variations of the fill factor and the conversion efficiency with the solar spectrum and temperature

According to the results shown in **Table 4** and the preceding figures, one notes that, for the three illuminations, while the temperature increases, the open circuit voltage ( $V_{oc}$ ) will decrease. This is the result of the reduction in the energy gap.

The increase in the temperature causes also a weak increase in the short circuit current. This result is explained by the improvement of the spectral response as we saw in the part (3.2).

As it is shown in Fig. 9, the fill factor undergoes a reduction with the increase in the temperature following the increase in the dark current (Fig. 7), and owing to the fact that the reduction in the open circuit voltage ( $V_{oc}$ ) is more significant with respect to the increase in the short circuit current, the conversion efficiency also will decrease.

#### 4. CONCLUSION

We have been developing a comprehensive model for a ZnO-SiO<sub>2</sub>-Si (N) solar cell, which consists of a wide range of parameters. The spectral response has been simulated for different solar spectrum and for temperature's range of 5 °C – 70 °C. Results show that our cell has a higher collecting efficiency for carriers generated by ultraviolet light. This result reveals one of the important advantages of MIS solar cells.

Results show also the improvement of the spectral response, especially in the range of longer wavelengths, with the increase in illumination intensity and of the temperature because of the increase in short circuit current and the improvement of the absorption in silicon for longer wavelengths.

The conversion efficiency of the cell decreases gradually with the temperature and it is proportional to the intensity of the incidental light. Thus we note that the effect of the increase in solar cell's temperature results a degradation of their performances. This is evidently the explanation of the observed drop of the conversion efficiency.

#### REFERENCES

- [1] S.M. Sze and K.K. Ng, '*Physics of Semiconductor Devices*', 832 p., Third Edition, John Wiley, Interscience, 2006
- [2] F. Sylvie, '*L'Oxyde de Zinc par Dépôt Chimique en Phase Vapeur comme Contact Electrique Transparent et Diffuseur de Lumière pour les Cellules Solaires*', Doctorat of Sciences Thesis, Lausanne, 2003.
- [3] K. Ellmer, A. Klein and B. Rech, '*Transparent Conductive Zinc Oxide: Basics and Application in Thin Film Solar Cells*', Springer, 2007.
- [4] K. Takahashi, A. Yoshikawa and A. Sandhu, '*Wide BandGap Semiconductors: Fundamental Properties and Modern Photonic and Electronic Devices*', Springer, 2007.
- [5] A.H.M. Shousha, '*Performance Characteristics of Thin Film MIS Solar Cells*', Solar & Wind Technology, Vol. 6, N°6, pp. 705-712, 1989.
- [6] H.C. Card and E. S. Yang, '*MIS Schottky Theory under Conditions of Optical Carrier Generation in Solar Cells*', Applied Physics Letters, Vol. 29, N°1, pp. 51 - 53, 1976.

- [7] J.P. Singh and R.S. Srivastava, '*Efficiency of  $\text{SnO}_2/\text{Si}$  Solar Cells*', Indian Journal of Pure and Applied Physics, Vol. 20, pp. 104 - 110, 1982.
- [8] H.C. Card and E.H. Rhoderick, '*Studies of Tunnel MOS Diodes I. Interface Effects in Silicon Schottky Diodes*', Journal of Physics D: Applied Physics, Vol. 4, N°10, pp. 1589 – 1601, 1971.
- [9] K. Bucher, J. Bruns and H.G. Wagemann, '*Absorption Coefficient of Silicon: An Assessment of Measurements and the Simulation of Temperature Variation*', Journal of applied Physics, Vol. 75, N°2, pp. 1127 – 1132, 1994.
- [10] R.C. Neville, '*Solar Energy Conversion, The Solar Cell*', Second edition, Elsevier 1995.
- [11] A. Laugier et J.A. Roger, '*Les Photopiles Solaires*', Technique & Documentation Lavoisier, 1981.
- [12] B.O. Seraphin, '*Solar Energy Conversion – Solid State Physics Aspects*' Topics in Applied Physics, Vol. 31, Springer, 1979.
- [13] H.J. Hovel, '*Semiconductors and Semimetals*', Edition R. K. Willardson, 1975.